



Aug 5, 2015

Fabrication of bulk iron nitride for energy conversion

Todd Monson*, Baolong Zheng†, Yizhang Zhou†,
Enrique Lavernia†, Siddharth Kulasekaran‡, Raja
Ayyanar‡, Charles Pearce*, Stanley Atcitty*

* Sandia National Laboratories

† University of California, Davis

‡ Arizona State University

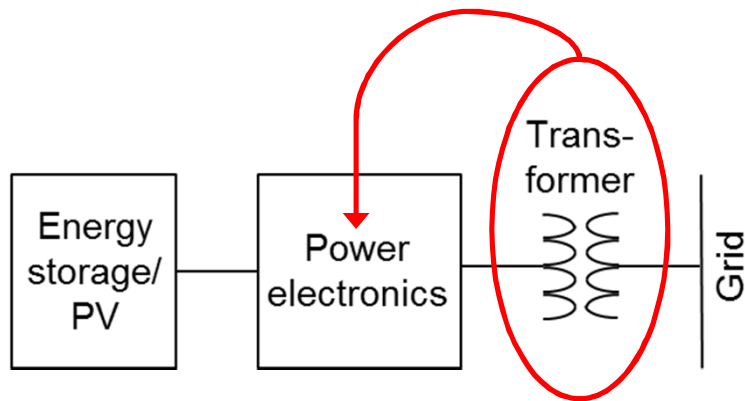
The authors acknowledge support for this work from Dr. Imre Gyuk and the Energy Storage Program in the Office of Electricity Delivery and Energy Reliability at the US Department of Energy



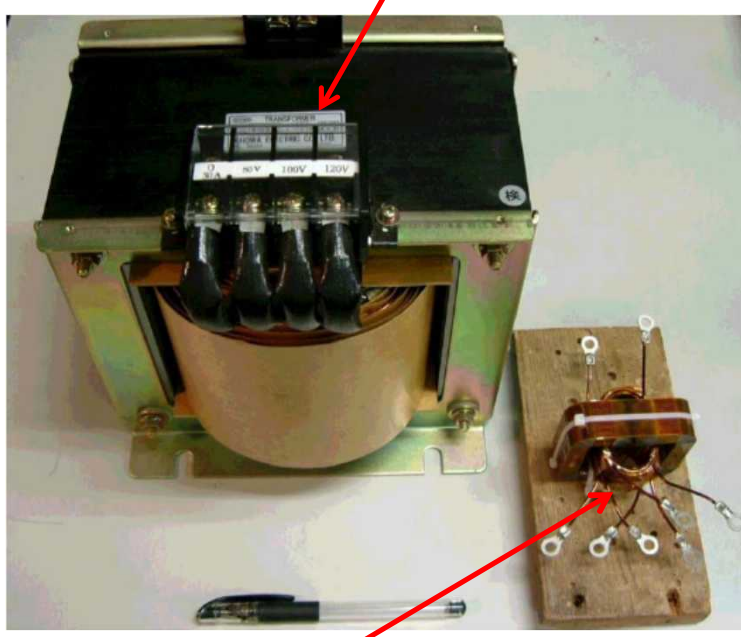
Sandia National Laboratories is a multi program laboratory managed and operated by Sandia Corporation, a wholly owned subsidiary of Lockheed Martin Corporation, for the U.S. Department of Energy's National Nuclear Security Administration under contract DE-AC04-94AL85000.



Benefits of a High Frequency Transformer



Line frequency (50 Hz) transformer



High frequency (20 kHz) transformer

- Integrate output transformer within power conversion electronics
- Leverage high switching speed, voltage, and temperature performance of WBG semiconductors
- Transformer core materials for high frequency transformers have been an afterthought (no current material meets all needs)

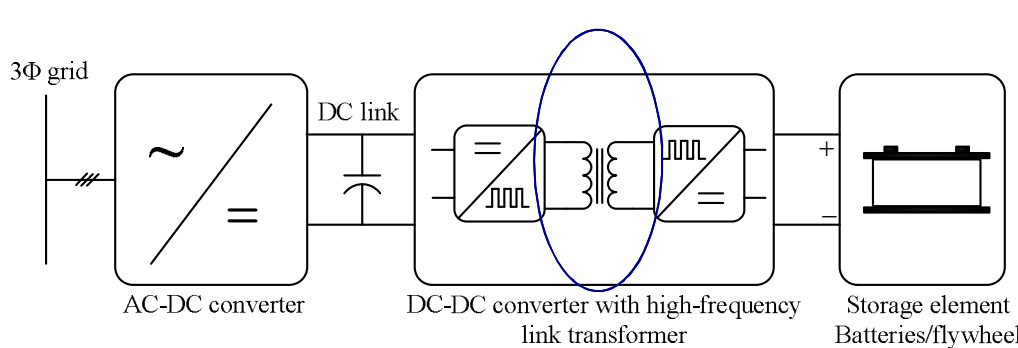
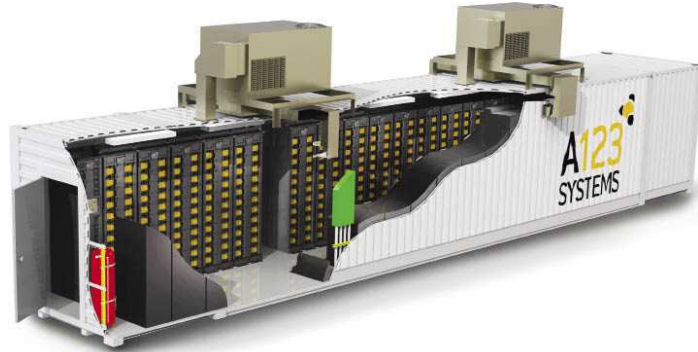
Material requirements:

- Low loss in 10-200 kHz frequency range
- High permeability (low coercivity)
- High saturation magnetizations
- Low magnetostriction
- High temperature performance
- Scalable manufacturing
- Affordable

Transportable Energy Storage and Power Conversion Systems (PCS)

Benefits of Energy Storage:

- Maintain power quality and reliability
- Improve stability and defer upgrades
- Improved agility and control (load leveling, power factor control, frequency and voltage regulation)
- Increase deployment of renewable generation



Benefits of Transportable Systems:

- Lower cost
 - PCS 20-60% of total energy storage system cost
- Modular design allows for fast installation at multiple sites

Power Transformer Market Analysis

Figure 12. Estimated Power Transformer Markets: United States v. China in 2010



Note: Different criteria used for the United States and China. For the United States, power transformers with capacity greater than or equal to 60 MVA are included in the data; for China, power transformers with capacity greater than or equal to 220 kV are included in the data.

Sources: USITC, 2011; China Transformer Net, 2010; China's Power Transformer Industry Report, Reuters, 2011.

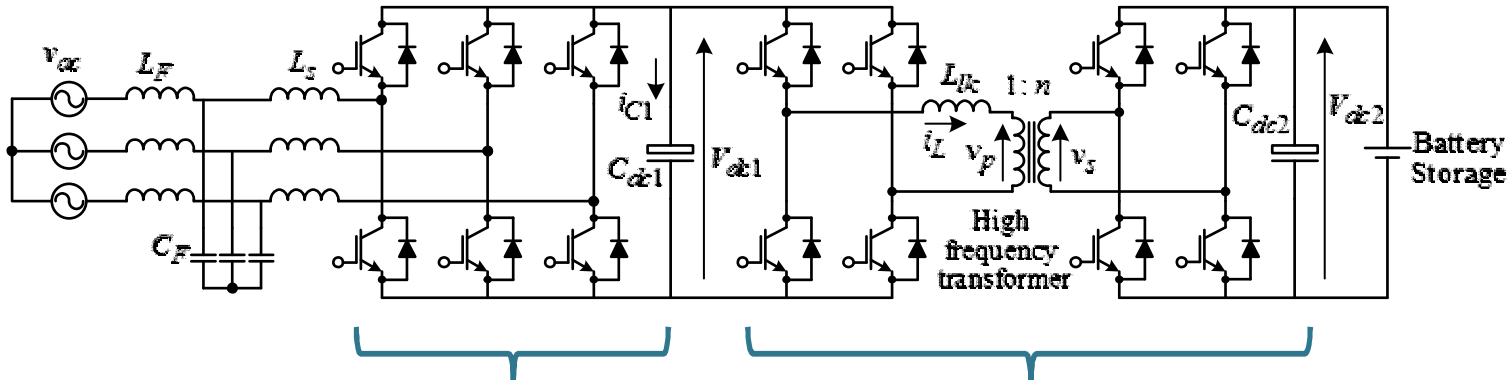
Transformer EMP Vulnerability



- **Geomagnetic storms couple very efficiently to long transmission lines**
- **Transformer can be driven to saturation, creating harmonics and reactive power**
- **Enough heat generated to melt copper windings**
- **Transformers the grid component that is hardest to replace**

Permanent damage to the Salem New Jersey Nuclear Plant GSU Transformer caused by the March 13, 1989 geomagnetic storm. Photos courtesy of PSE&G.

High Frequency Link Power Conversion System Configuration

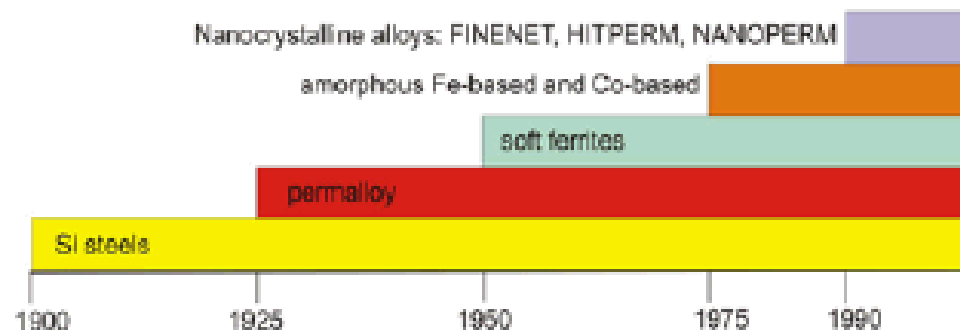


- Optimal switching frequency based on the losses at this stage

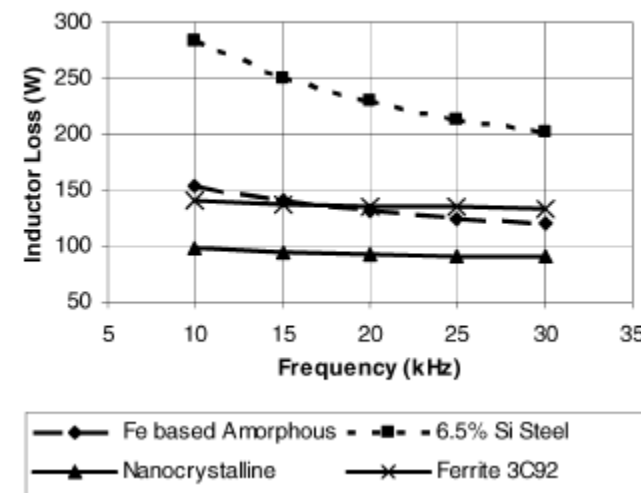
Volume occupied by heat sinks and non-magnetic components were not considered !!

- Optimal switching frequency based on:
- Switching and conduction losses in the switch
- Volume of the transformer
- Losses in the transformer
 - Copper losses in transformer windings
 - Core losses of the transformer

Development of Soft Magnetic Materials



L.A. Dobrzański, M. Drak, B. Ziębowicz, Materials with specific magnetic properties, Journal of Achievements in Materials and Manufacturing Eng., 17, 37 (2006).

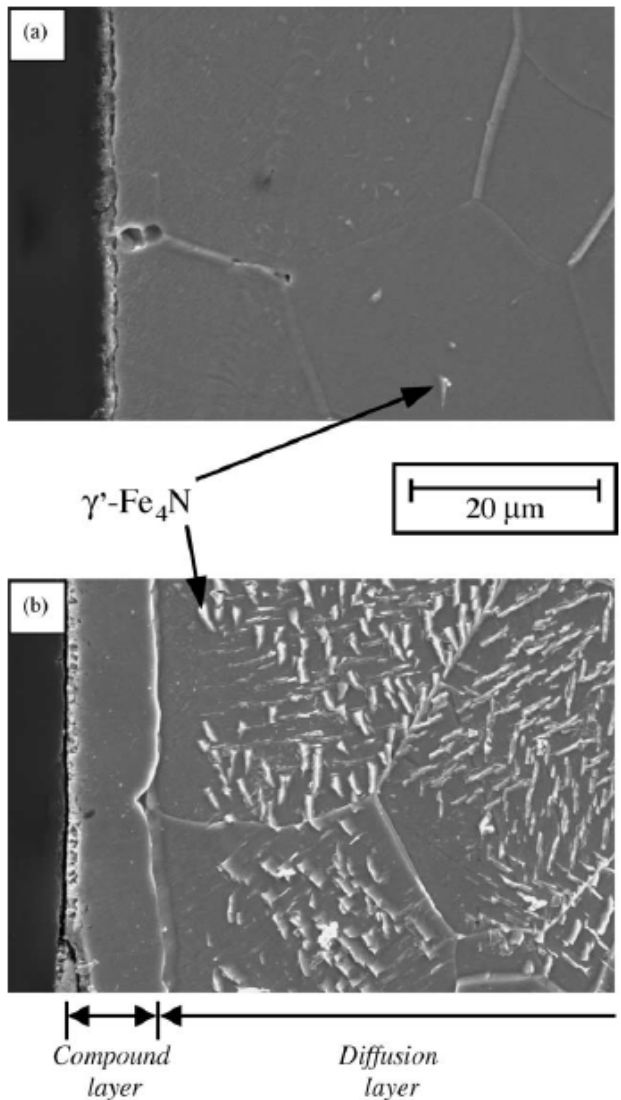


B.J. Lyons, J.G. Hayes, M.G. Egan, Magnetic Material Comparisons for High-Current Inductors in Low-Medium Frequency DC-DC Converters, IEEE, 71 (2007).

Magnetic Material	J_s (T)	$\rho(\mu\Omega\cdot m)$	Cost
VITROPERM (Vacuumschmelze)	1.20	1.15	High
Metglas 2605SC	1.60	1.37	High
Ferrite (Fexxocube)	0.52	5×10^6	Low
Si steel	1.87	0.05	Low
γ' -Fe ₄ N	1.89	~200	?

- Little or no development of new magnetic materials since the early 1990s!
- Nanocrystalline alloys low loss but magnetizations low when compared to bulk iron ($P_{max} \sim f \cdot \Delta B \cdot A_{core} \cdot A_{Cu} \cdot I_{sat}$ $I_{sat} = B_{sat} \cdot I_m / \mu \cdot n$ $E_{rms} = 4.44 \cdot f \cdot n \cdot A \cdot B_{sat}$)
 * ΔB and I_{max} also limited by ΔT (max temp. rise)

In House Synthesis of Raw Materials: Electrochemical Nitriding of Iron



- Growth of γ' -Fe₄N demonstrated by Japanese electrochemists
- Formed γ' -Fe₄N at the surface of Fe(0) electrode using Li₃N as nitride source
- Demonstrates electrochemical synthesis of iron nitride possible
- Our goal is to demonstrate autonucleation of iron nitride with flowing N₂

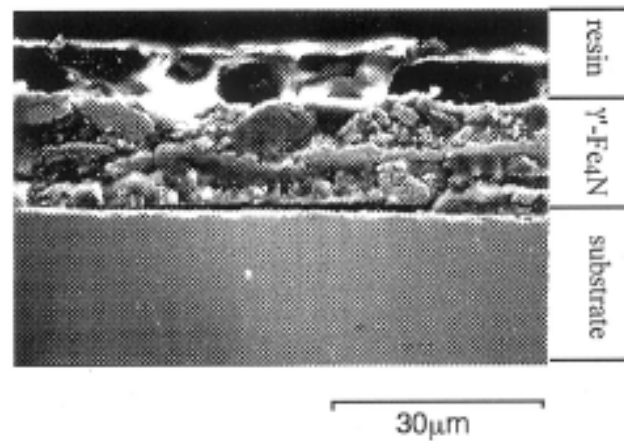
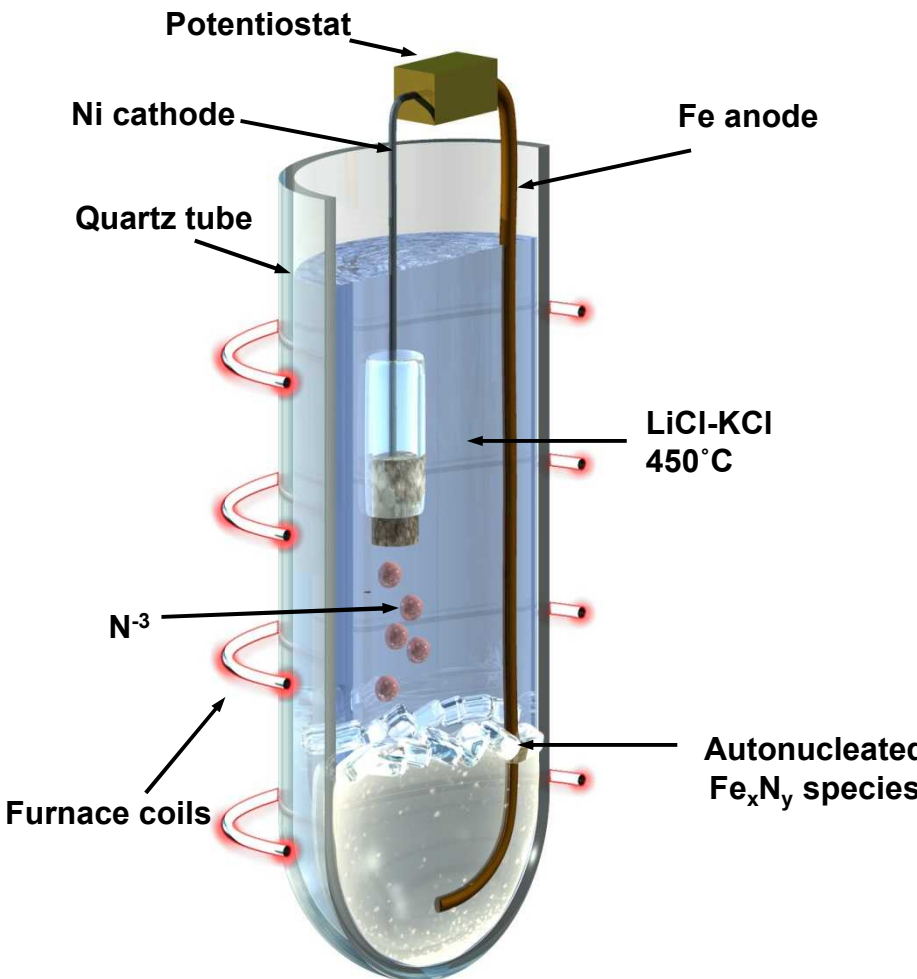


Fig. 10. Cross-sectional SEM image of iron electrode after potential pulse electrolysis for 1 h.

Electrochemical Solution Growth of Magnetic Nitrides



- Not electroplating!!!!
- Molten salt solution growth of GaN developed and patented at Sandia
- Create ionic precursors electrochemically
- Use salt transport to deliver precursors
- Increase growth rate through flux of reactants (increase currents, N_2 flow also has an effect)
- Can control oxidation state of transition metal
- Produces high quality material



Precursors can be replenished as they are consumed
Advantage: Continuous, isothermal or steady-state growth

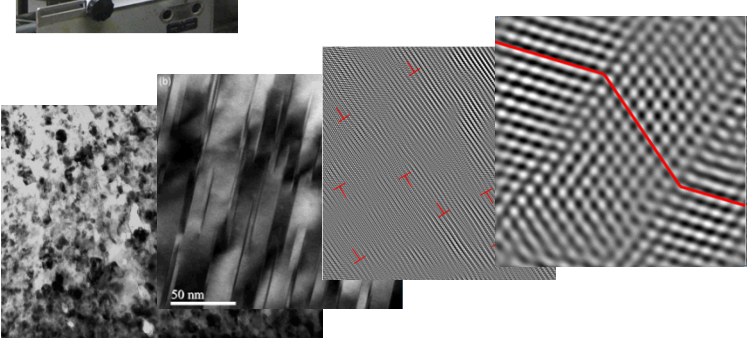
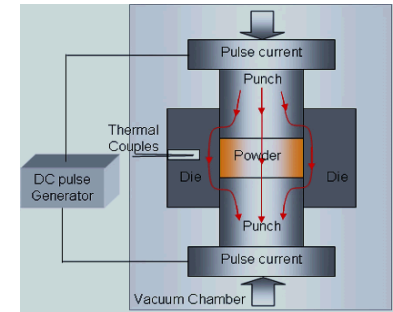
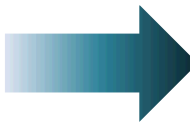
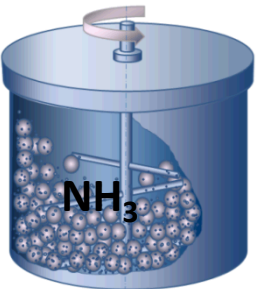
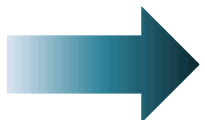
U.S. Patent Filed November 2014

Cryomilling of Iron Powders



U.S. Patent Filed January 2015

Synthesis of dense nanocrystalline iron nitrides using a two-step reactive milling and high pressure spark plasma sintering (SPS).



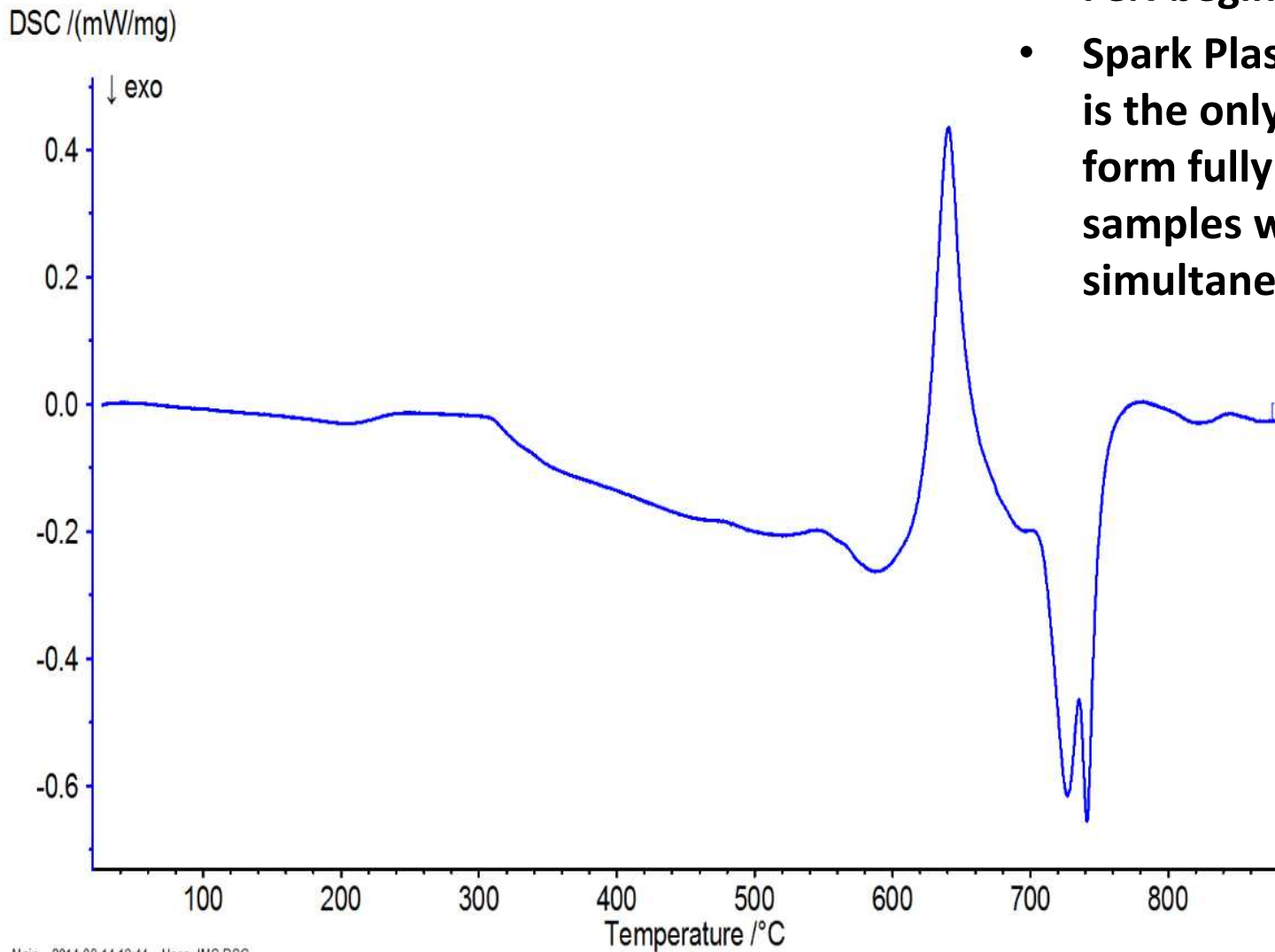
- Smaller the grain size, bigger the tendency to grain growth.
- Thermal stability of NC depends on lattice defects stored between and within grains.

▪ Cryomilling can be used to fabricate nanocrystalline (NC) Fe powder with large amounts of vacancies, grain boundaries, and dislocations, which serve as fast diffusion pathways for nitrogen atoms, and create new reactive surfaces through which the nitriding process of iron can be enhanced.

▪ SPS is effective at achieving fully dense NC materials, due to lower sintering temperature and shorter time required

▪ Pressure can additionally limit grain growth and help lead to full densification.

Differential Scanning Calorimetry (DSC) of Fe_4N

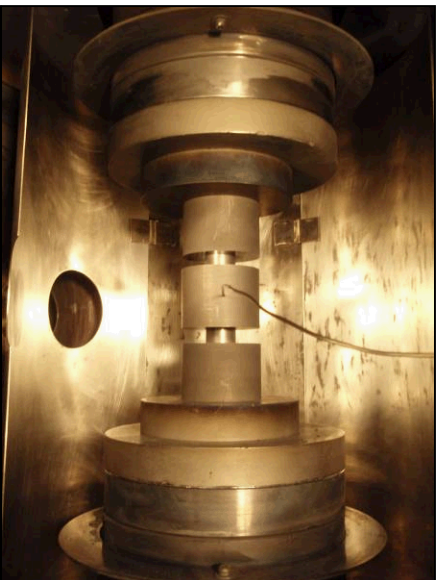


- Decomposition of sintered FeN begins $\approx 600^\circ\text{C}$
- Spark Plasma Sintering (SPS) is the only viable route to form fully dense bulk Fe_4N samples without simultaneous decomposition

Spark Plasma Sintering (SPS)

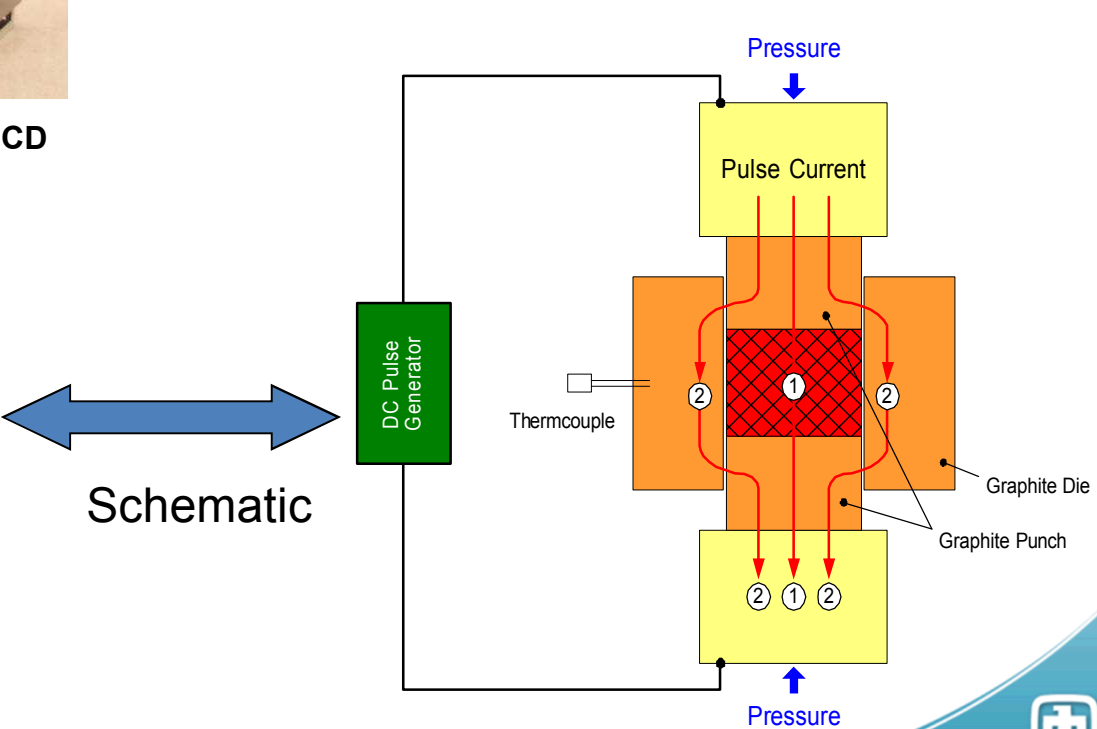


SPS Model: SPS-825S Dr. Sinter® at UCD

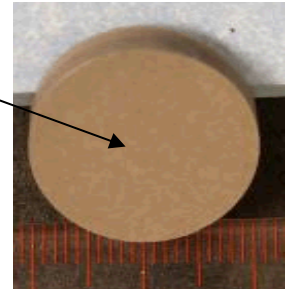


SPS Synthesis Chamber

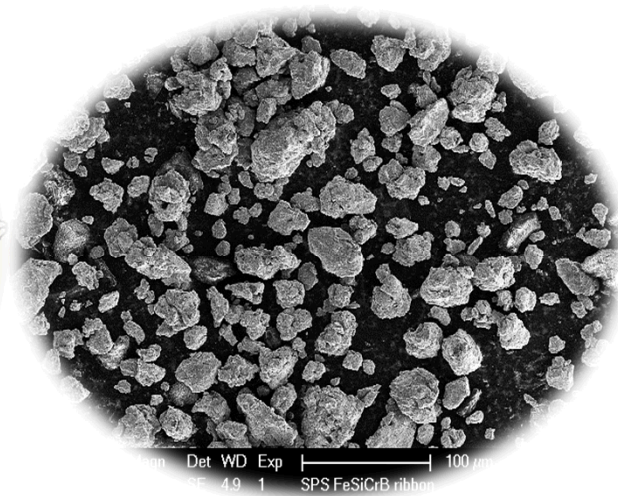
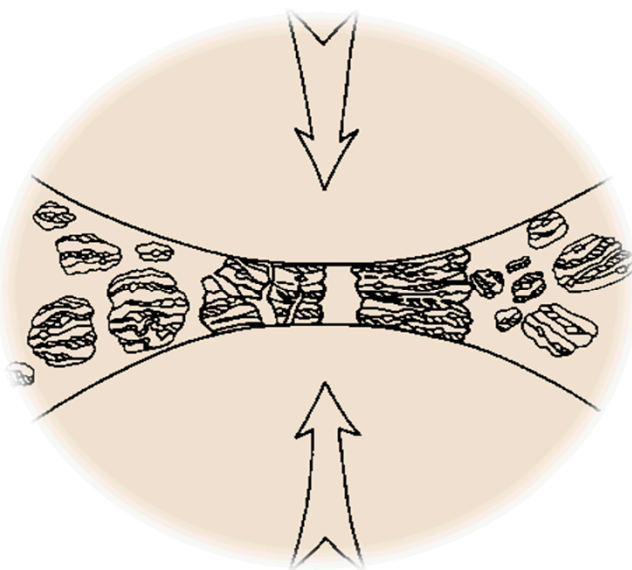
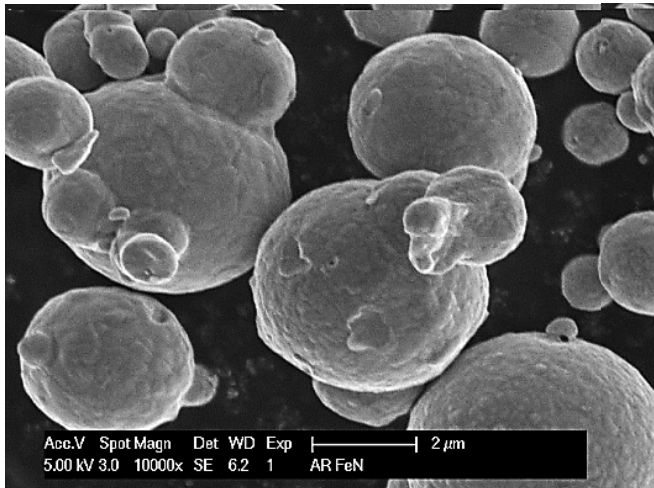
Schematic



End Product



Materials Pre-Processing

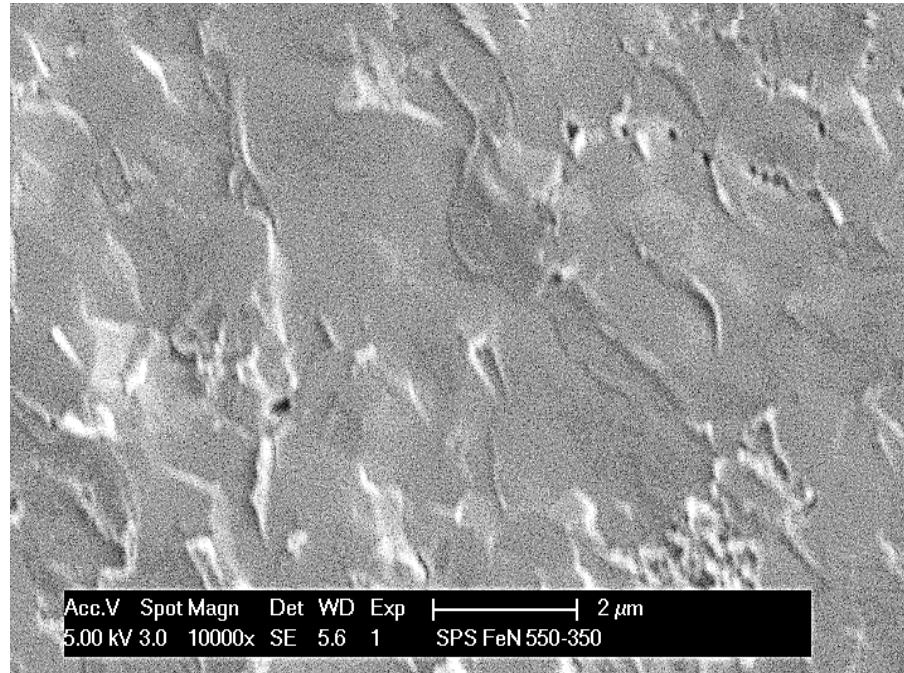
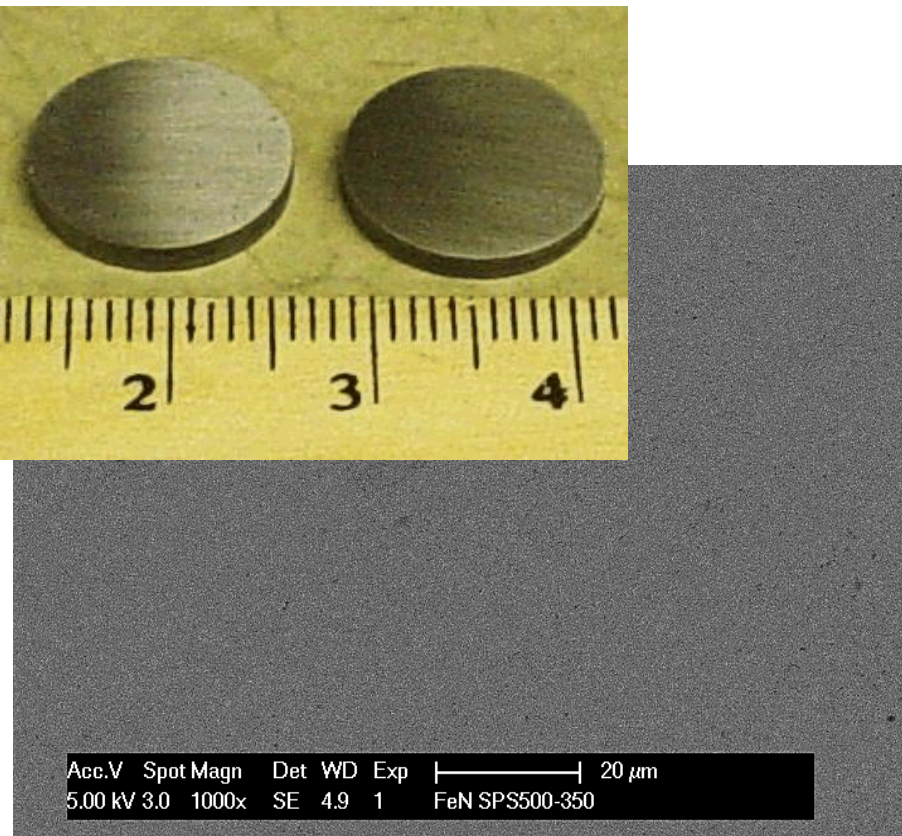


Starting Fe_xN_y Powder

Mechanical Milling

Milled FeN Powder

SPS consolidation



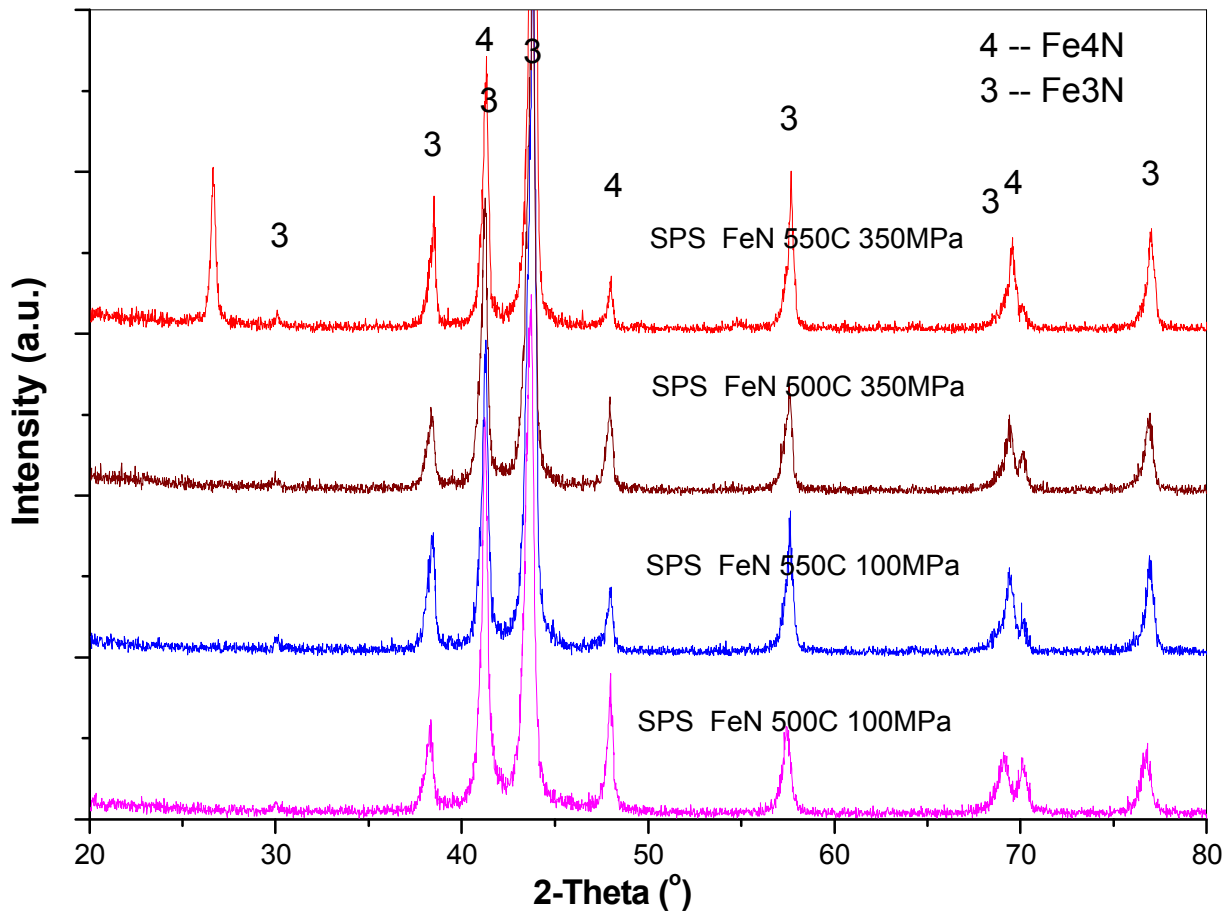
- SPS sintering: 550°C, 350 MPa, 3 min.
- High densities achieved in the SPSed iron nitride samples

TEM of SPSed FeN

- FeN particles were well consolidated with little porosity
- The grain size of SPSed FeN ranged from 200 nm to 1 μm .

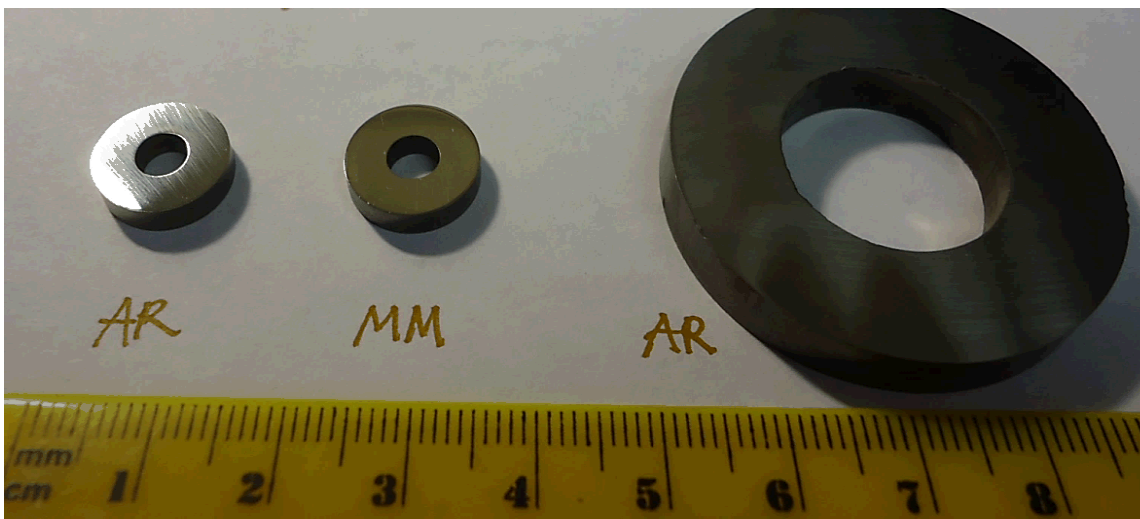
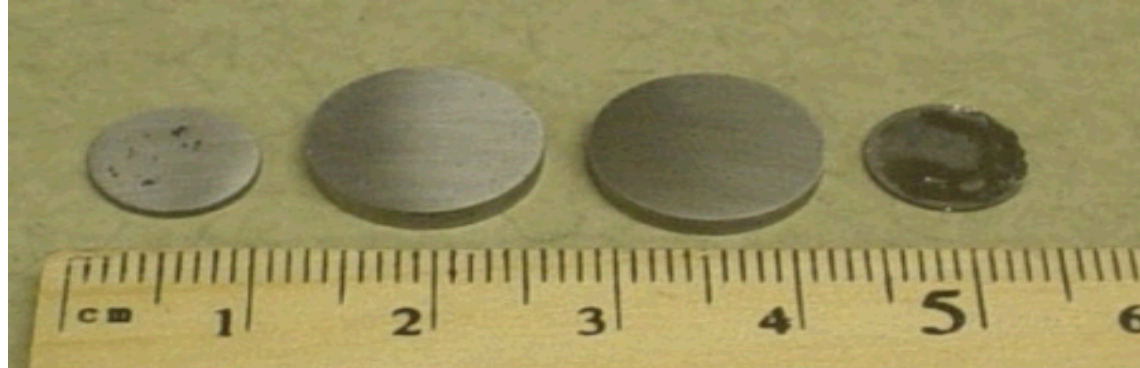


XRD of SPSed FeN



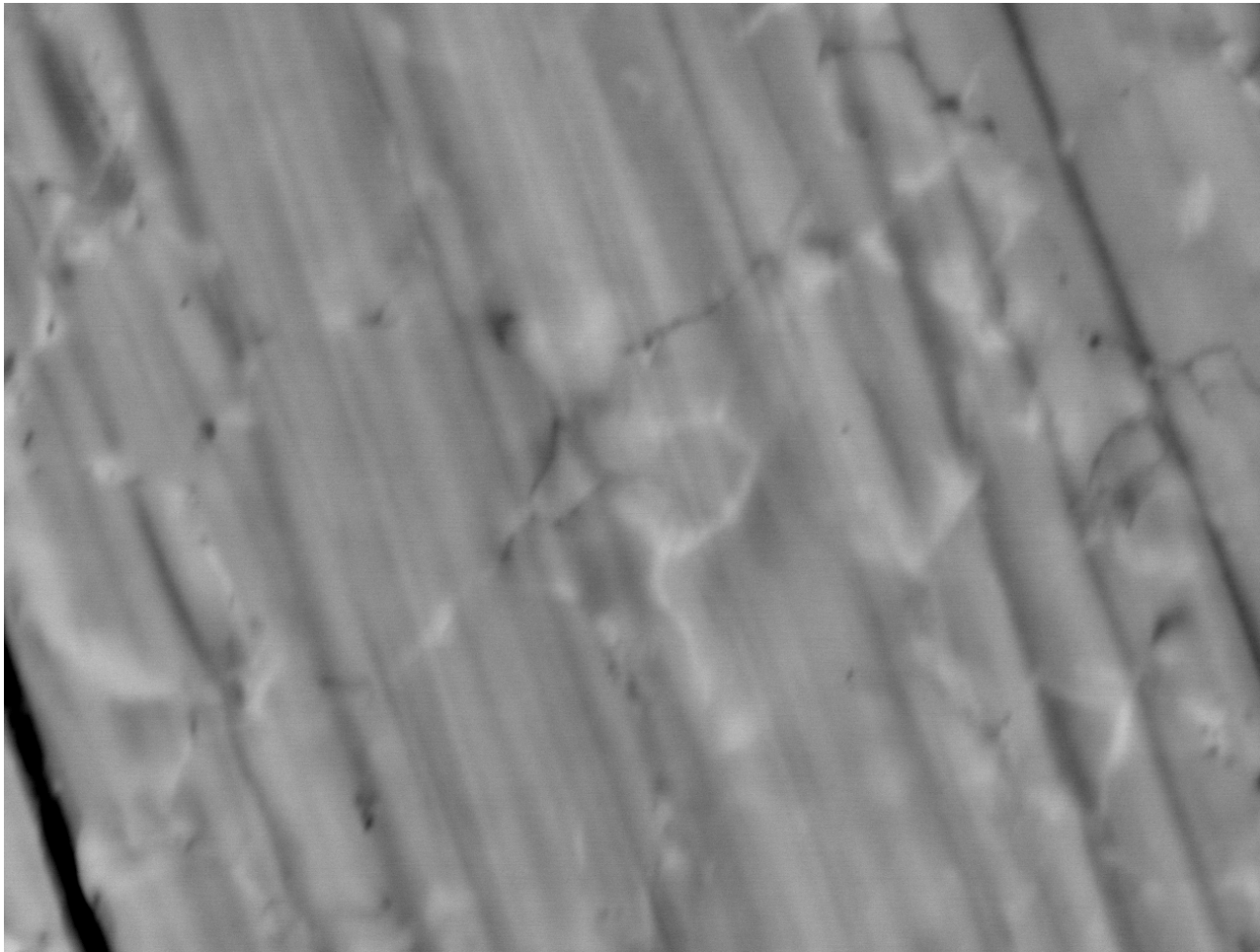
- XRD of FeN samples produced using different SPS conditions
- Raw powders contained a mixture of Fe_3N and Fe_4N

SPSed Samples and Net-Shaping



- Can sinter toroids and other complex shapes directly (net-shaping), eliminating the need for machining
- Toroids will be wound and tested under this fiscal year's effort

Toroid Surface SEM and EDS



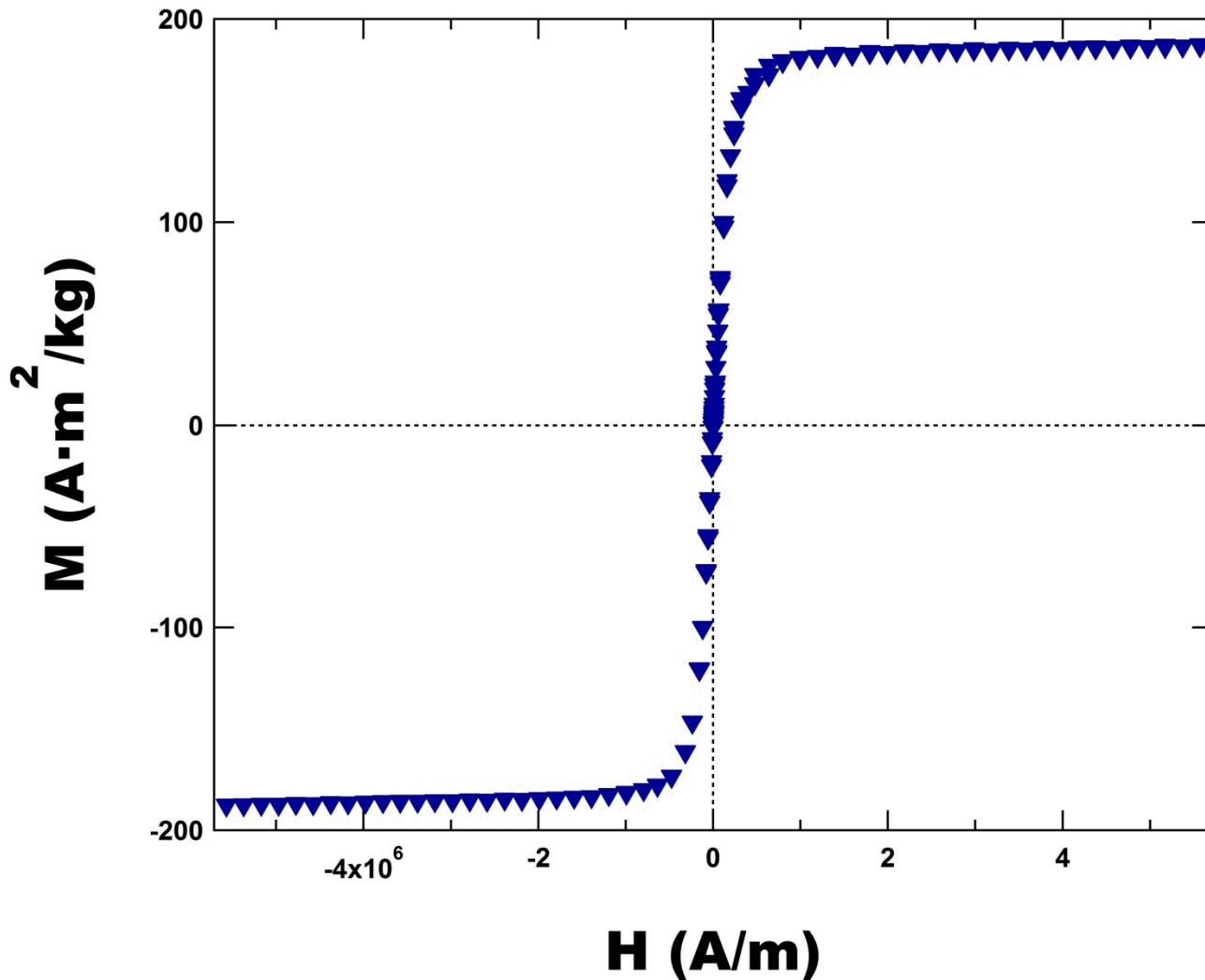
- Small variation in composition between grain boundary and center
- Grain center stoichiometry $\approx \text{Fe}_4\text{N}$
- Grain boundary is ≈ 3 Atomic% richer in iron

*SEM/EDS analysis completed by Dick Grant (SNL)

X 10,000 20.0kV COMPO NOR 1 μm JEOL 11/10/2014
WD 11.0mm 11:08:26

Location	Fe (Atomic %)	N (Atomic %)
Grain center	81.3	18.7
Grain boundary	84.2	15.8

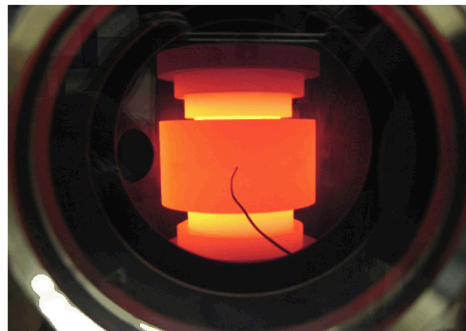
Magnetic Results



- Fe_4N SPSed at 550°C and 100 MPa achieved an M_{sat} of $188 \text{ A}\cdot\text{m}^2/\text{kg}$.
- Predicted M_{sat} of bulk γ' - Fe_4N is $209 \text{ A}\cdot\text{m}^2/\text{kg}$ (Fe is $217 \text{ A}\cdot\text{m}^2/\text{kg}$)
- Negligible coercivity

Conclusions & Future Work

- **γ' -Fe₄N has the potential to serve as a new low cost, high performance transformer core material**
 - $M_{sat} >$ Si steel
 - Increased current and field (and therefore power) carrying capability
 - Resistivity 200X greater than nanocrystalline and amorphous alloys
 - Only requires low cost and abundant elements (Fe & N)
- **The fabrication of bulk γ' -Fe₄N using SPS has been demonstrated**
 - SPS can consolidate iron nitrides without material decomposition
 - Parts can be fabricated directly using net-shaping
- **SPS processing parameters are being modified to improve phase purity, nanoscale grain structure, and magnetic performance**
- **Parallel development of multiple routes to γ' -Fe₄N raw powders**



Acknowledgements

SEM/EDS: Dick Grant (SNL)

The authors acknowledge support for this work from Dr. Imre Gyuk and the Energy Storage Program in the Office of Electricity Delivery and Energy Reliability at the US Department of Energy



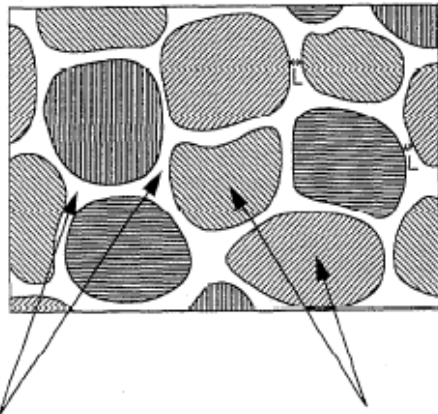
Extra Slides

Military Microgrid



- Almost identical challenges facing modernization of civilian electrical grid
- Desire to deploy systems in a small number of ISO containers
 - Requirement to reduce space of power conversion system

Nanocrystalline Alloy Materials & Manufacturing

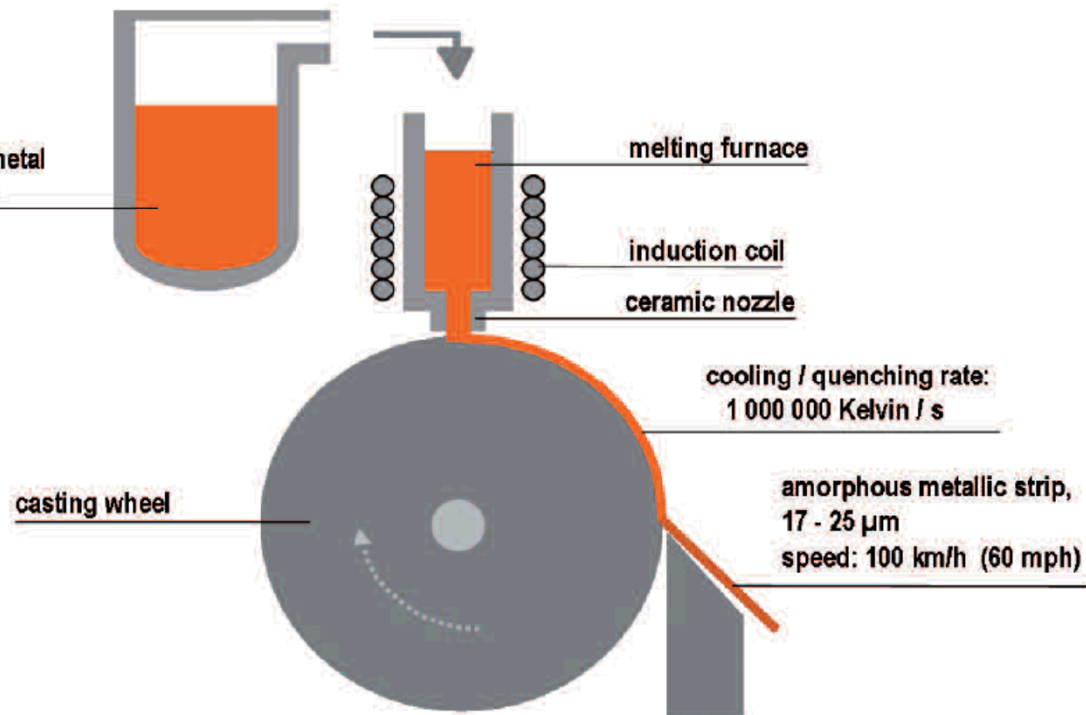


Intergranular amorphous phase with high T_c and high thermal stability due to large amounts of M and B elements.

Nano-scale α -Fe grains with small λ due to small amounts of M and B elements.

“NANOPERM”

A. Makino, et. al., Nanocrystalline Soft Magnetic Fe-M-B (M = Zr, Hf, Nb) alloys and their applications, Mat. Sci. and Eng., A226-228, 594 (1997).



VITROPERM (Vacuumschmelze)

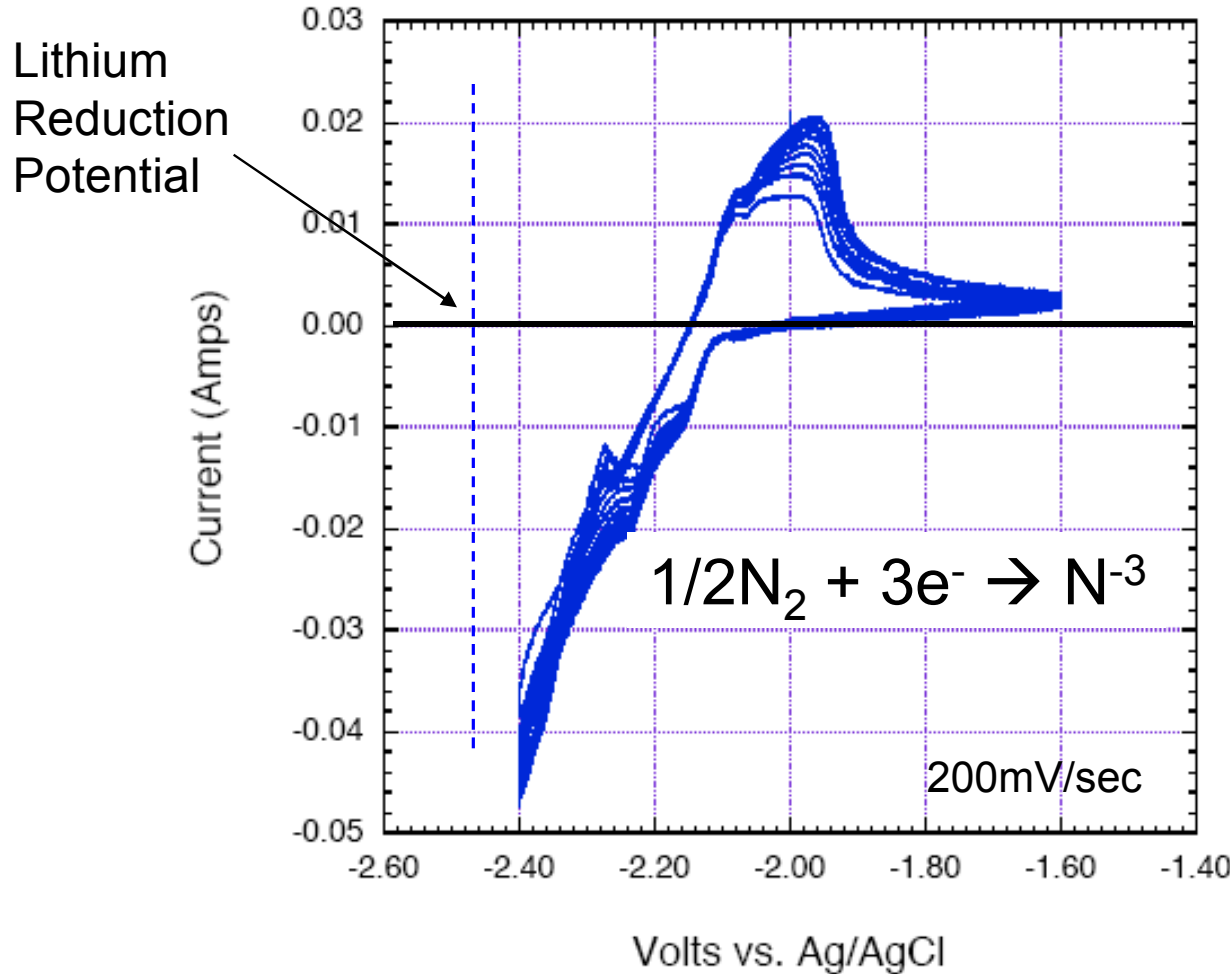
- Complex stoichiometries including Fe, Co, and other inactive elements such as B, Zr, Hf, Nb, Cu, Mo, Si, C
- Time consuming and high temperature processing → costly!
- Substantial inactive material to form a low loss nanocrystalline structure and limit eddy current loss
- Material produced in tapes and often combined with laminations

Other Magnetic Nitrides of Interest

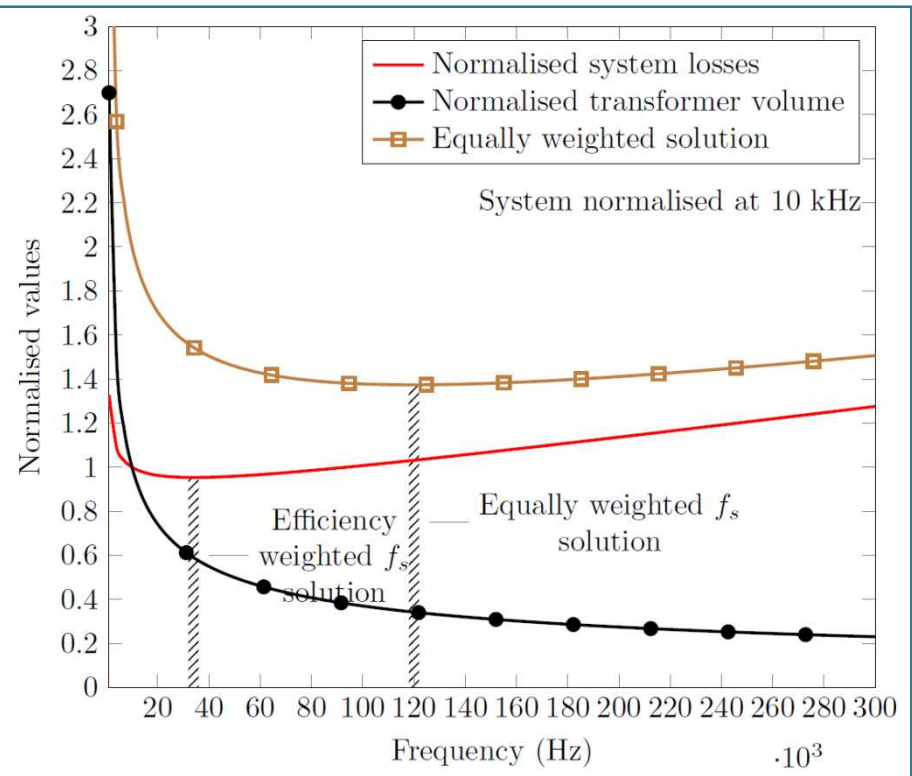
Material	Phase	σ_s (Am ² /kg)	J_s (T), if available	T_c (K)	H_c (A/m)
FeN	rocksalt (fcc or fct)	209			
γ' -Fe ₄ N	antiperovskite-like	209	1.89	769	460
α'' -Fe ₁₆ N ₂	tetragonal	230 - 286	2.3	810	
α'' -Fe ₉₀ N ₁₀		230			
g-C ₄ N ₃	graphitic	62			
MnN	rocksalt	194-308			4000
α -Fe	bcc	217	2.15	1044	70

- Nitrides will have higher resistivities than current transformer core materials and will not require laminations of inactive material to mitigate eddy current losses**

Example of Nitrogen Gas Reduction Cyclic Voltammograms

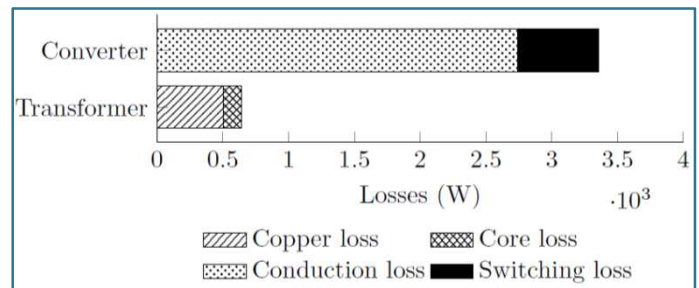


Optimum Frequency with SiC MOSFETs



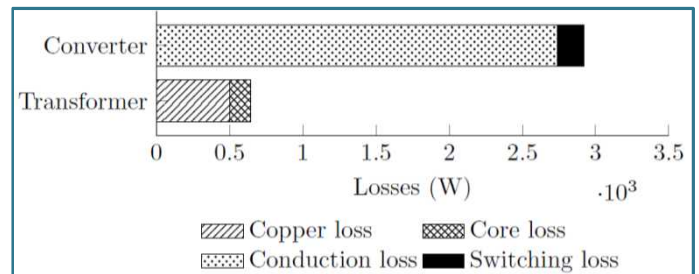
Equally weighted solution:

The converter has optimal solution at a frequency of **120 kHz** with equal weights on volume and losses

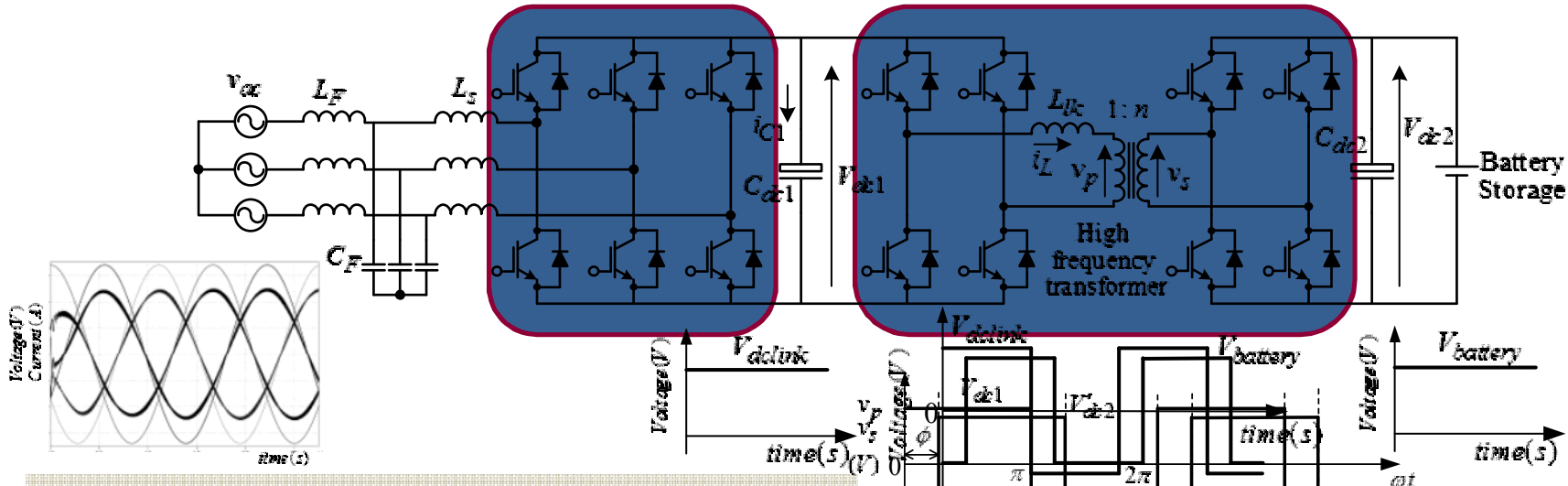


Efficiency driven solution:

The optimal solution for minimum loss condition is **35 kHz**



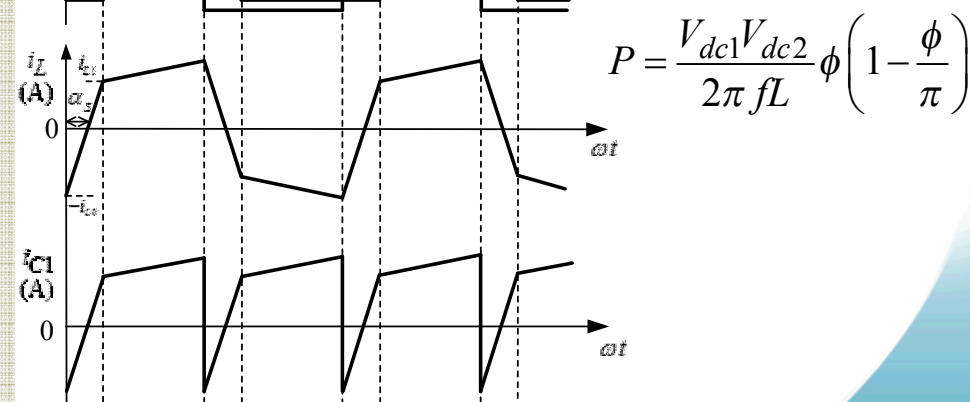
System Configuration



Parameters

Power Level	250 kW
Maximum RMS current	370 A
Maximum voltage	$1100 \text{ V} \pm 10 \text{ \%}$
Transformer core material	Ferrite
Transformer turns ratio	1:1
Transformer leakage inductance	$18 \text{ }\mu\text{F}$
Snubber capacitance	20 nF
DC Capacitor (Input/ Output)	4.4 mF

Specifications



$$P = \frac{V_{dc1}V_{dc2}}{2\pi fL} \phi \left(1 - \frac{\phi}{\pi} \right)$$

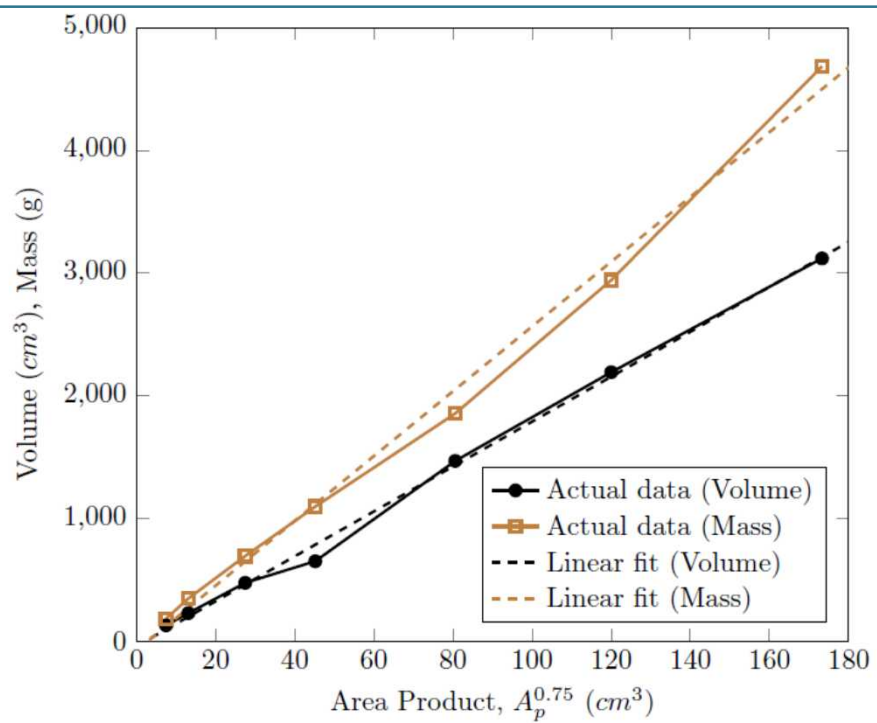
Loss and Volume Estimation

Transformer Volume Estimation:

Power handling capacity of the cores are identified by Area product, A_p (cm⁴)

$$A_p = \frac{S}{k_w J_{max} \Delta B_{max} f}$$

Area Product vs Volume, Mass



A_c = Area of the core

A_w = Window area

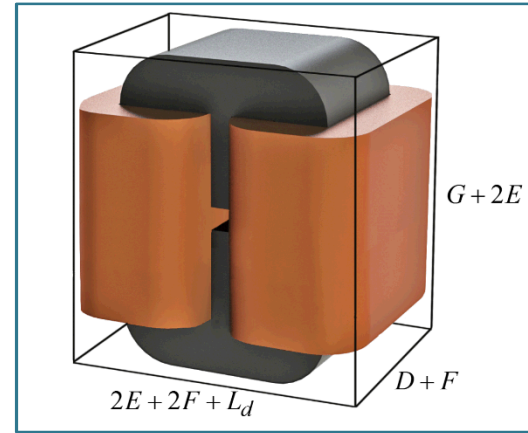
S = Total volt-amp rating of the transformer (VA)

k_w = window utilization factor

J_{max} = Current density (A/cm²)

ΔB_{max} = flux density (T)

f = switching frequency (Hz)



$$\text{Volume} = K_v A_p^{0.75}; K_v = 18.302$$

$$\text{Mass} = K_p A_p^{0.75}; K_p = 26.41$$

$$\text{Volume} = \frac{8.328 \times 10^6}{\Delta B^{0.75} f^{0.75}} \text{cm}^3$$

Transformer Losses

Transformer copper loss:

$$P_{cu} = 2K_r \frac{N_{pri} \rho l}{A_{cond}} I_{rms}^2$$

$$N_{pri} = \frac{V_{pri}}{\Delta B_{max} A_c f}$$

$$P_{cu} = \frac{288475.68}{\Delta B^{0.75} f^{0.75}} W$$

Mean turns length :

$$l = 2(E + D) + \pi F/2$$

where,

$$N_{pri} = \frac{1703.1}{\Delta B^{0.5} f^{0.5}}; R_{dc} = \frac{1.0536}{\Delta B^{0.75} f^{0.75}}$$

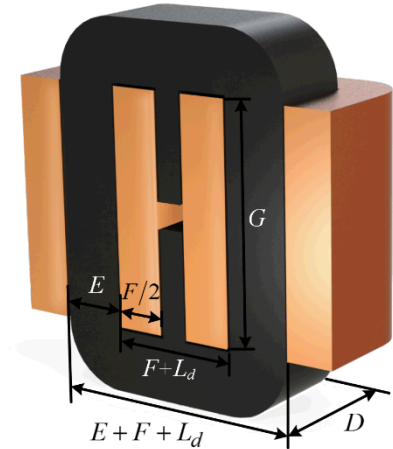
Transformer Iron loss:

$$P_{fe} = \left(k f_{eq}^{\alpha-1} \hat{B}^{\beta} \right) f \quad \leftarrow \text{Modified Steinmetz equation}$$

$$f_{eq} = \frac{2}{\Delta B^2 \pi^2} \int_0^T \left(\frac{dB}{dt} \right)^2 dt$$

The total iron losses in a 3C93 ferrite core is

$$P_{fe} = 4.77 f^{0.6} \Delta B^{2.45}$$



Optimal flux density

$$\begin{aligned} P_T &= P_{cu} + P_{fe} \\ &= \frac{288475.68}{\Delta B^{0.75} f^{0.75}} + 4.77 f^{0.6} \Delta B^{2.45} \end{aligned}$$

$$\frac{dP_T}{dB}(f = \text{const}) = 0$$

$$B_{opt} = \frac{21.557}{f^{0.425}}$$

Two applications of high frequency high power transformers (HFHPTs)

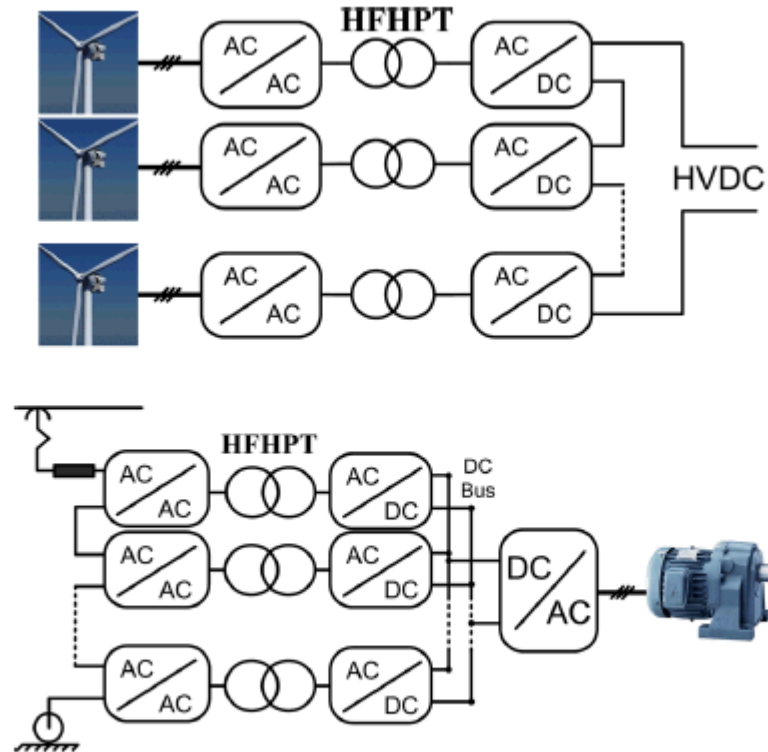


FIG. 1. Two main applications of high power converters with HFHPTs, (top) offshore wind farm and (bottom) traction converter.

E. Agheb, et. al., Core loss behavior in high frequency high power transformers-II: Arbitrary excitation, J. of Renewable and Sustainable Energy, 4, 033113 (2012).

Grid-connected inverter with high-frequency DC link

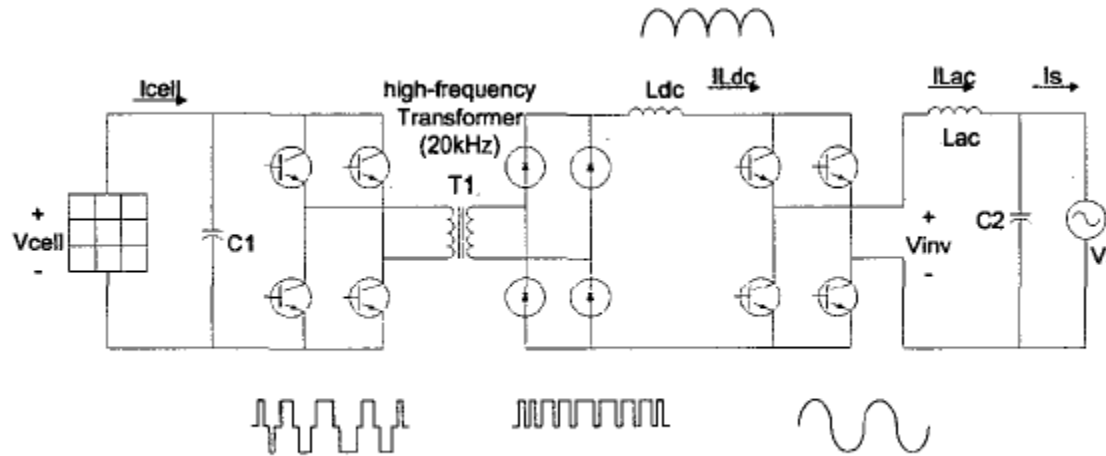


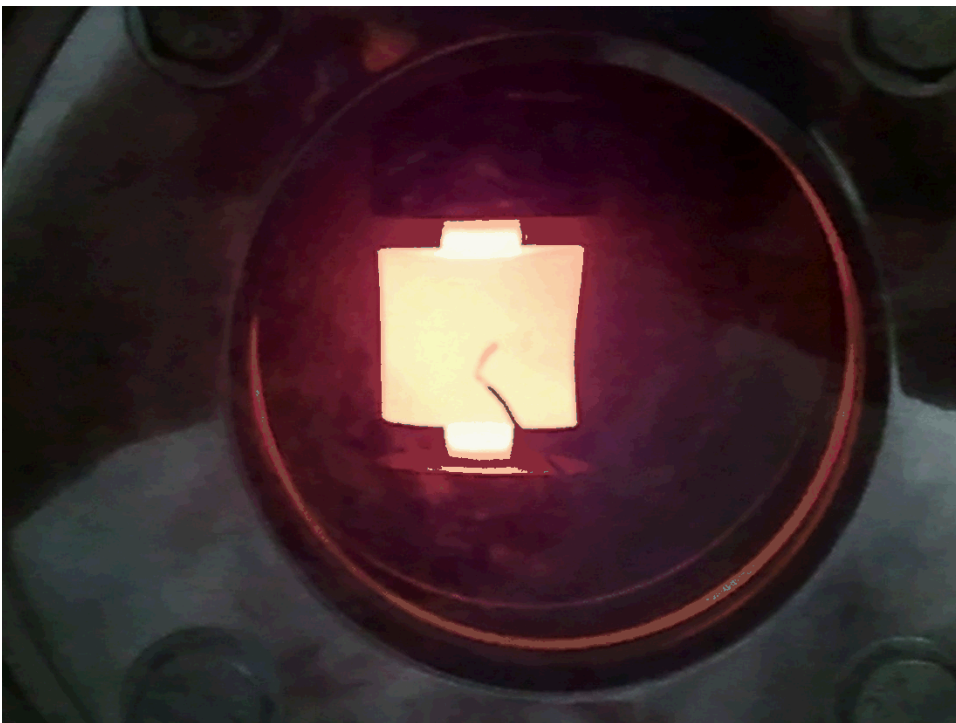
Fig. 1. Grid-connected inverter with high-frequency DC link.

Y. Jung, et. al., High-frequency DC link inverter for grid-connected photovoltaic system, IEEE, 1410 (2002).

Spark Plasma Sintering (SPS)



- DC current
 - ON(1-99 ms)/OFF(1-9 ms) pulse
- Surface activation
 - Electromigration
- Short time
 - 5~30 min
 - Max. heating rate ~ 400 °C/min
- SPS-825S
 - Max. force: 250 kN
 - Max. current: 8000 A
 - Sample dimension: $\Phi 80$ mm
- Offers the ability to fine tune grain size in sintered devices



SPS for Manufacturing Ceramics

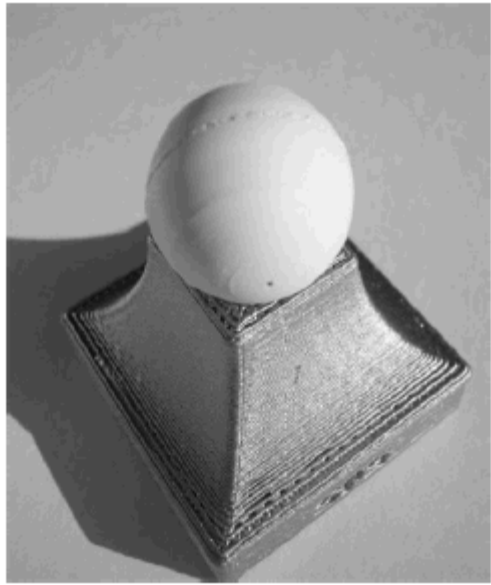


Fig. 9. Al_2O_3 sphere obtained in one single step by SPS.^[63]

J. Galy, Private Communication, 2007.

Hungría et. al., Adv. Eng. Mater. Vol. 11 (2009) 616
DOI: 10.1002/adem.200900052

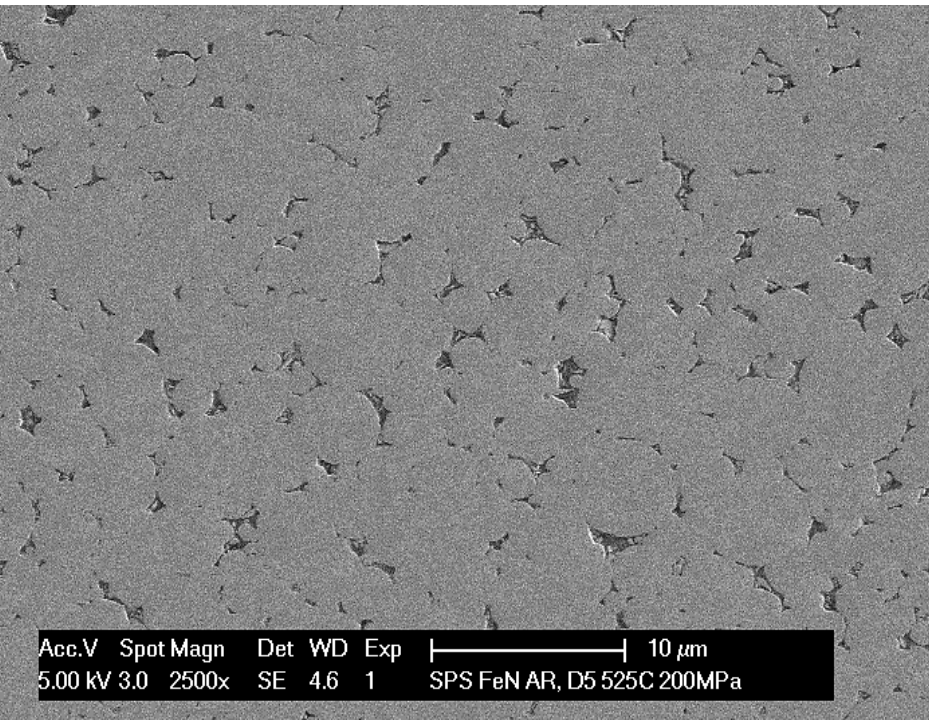
SPS System Manufacturers:

- Fuji Electronic Industrial Co. (Japan)
- FCT Systeme GmbH (Germany)
 - Can make components up to 500 mm (~20") in diameter
- Thermal Technology LLC (Santa Rosa, CA)

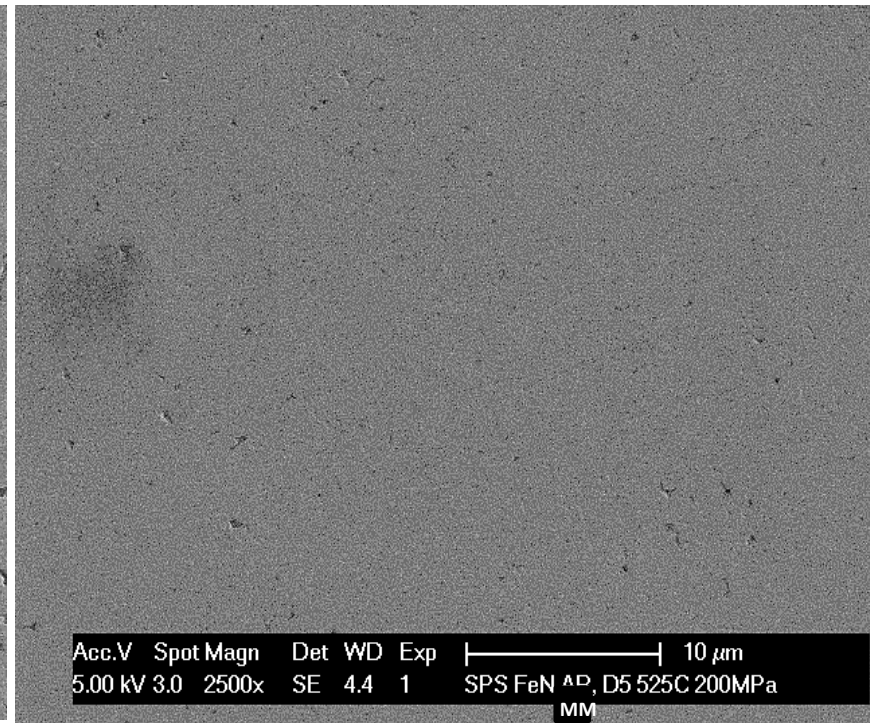
- Size of equipment increasing to accommodate commercial needs
- Technology for continuous SPS under development
- A large number of companies have acquired SPS but often request this info to not be made public to maintain a competitive advantage

SEM of SPSed FeN samples, (Ø5mm, 525°C, 200MPa)

W/ as-received FeN powder

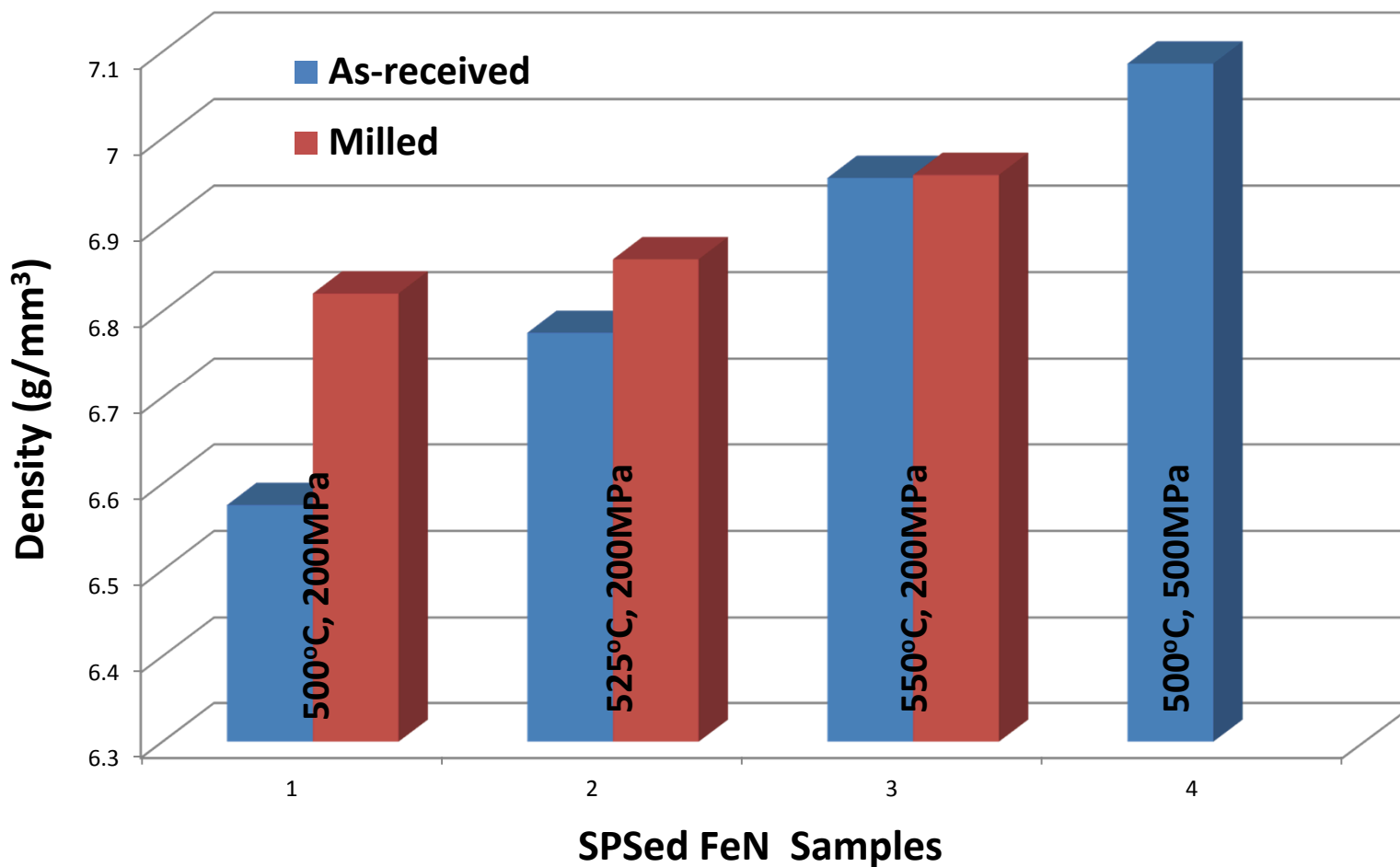


W/ milled FeN powder



- **Milled FeN powder produces more uniform and dense SPSed billets**
 - **Higher packing density with smaller particle size**
 - **Increased diffusion ability with smaller grain size of milled powder**

Density of SPSed FeN samples



- Density increases with increasing SPS temperature and pressure;
- Higher degree of variation in the density of the SPSed FeN with as-received powder
- Milling can improve density and uniformity of the consolidated FeN from powder